Asian Journal of Chemistry; Vol. 28, No. 12 (2016), 2788-2792

ASIAN JOURNAL OF CHEMISTRY

http://dx.doi.org/10.14233/ajchem.2016.20124

Molecular Insights into Interactions of Human Islet Amyloid Polypeptide with Lipid Membranes using Atomic Force Microscopy and Fluorescence Microscopy

M.B. DIVAKARA[1,2], M.S. SANTOSH[1,*], C.R. RAVI KUMAR[3], B.L. DHANANJAYA[4] and N. REDDY[1]

[1]Centre for Incubation, Innovation Research and Consultancy, Jyothy Institute of Technology, Tataguni, Off Kanakapura Road, Bengaluru-560 082, India
[2]Visvesvaraya Technological University-Research Resource Centre, Jnana Sangama, Belagavi-590 018, India
[3]Department of Basic Sciences, East West Institute of Technology, Bengaluru-560 091, India
[4]Toxicology and Drug discovery Unit, Centre for Emerging Technologies, Jain Global Campus, Jakkasandra Post, Kanakapura Taluk, Ramanagara District-562 112, India

*Corresponding author: E-mail: santoshgulwadi@gmail.com

Received: 6 June 2016; *Accepted*: 30 July 2016; *Published online*: 1 September 2016; AJC-18082

Type 2 diabetes mellitus (T2DM) is a global disease, in which the human amylin protein aggregates to form human islet amylin polypeptide (hIAPP) non-fibrils that are cytotoxic to pancreatic β-cells. The transformational change in hIAPP is accompanied by amorphous amyloid deposits on planar lipid membranes where in ordered and disordered membranes differ in the process of oligomerization, which is consistent with pathological findings in diabetic subjects. Such a transformational change results in the formation of non-fibrils, which are cytotoxic. In this study, with the use of atomic force microscopy (AFM) and fluorescence microscope (FM), we investigate the surface interactions and sequential conversion of hIAPP from small oligomers to mature hIAPP non-fibrils. It is observed that prolonged incubation under 25 °C, prohibits the fibrillar extension and permits formation of non-fibrillar peptide aggregates. These atomic force microscopy and fluorescence microscope techniques help in differentiating the oligomer formation better in real time and indicates how oligomer finally leads to changes in membrane morphology. Hence, this combined (AFM and FM) approach offers new molecular insights into the etiology of diabetes that could be extended to investigate amylin aggregation, oligomerization and amyloid non-fibril formation *in vivo* at a subcellular resolution.

Keywords: Amyloid, IAPP, Type 2 diabetes, Oligomer, Peptide-membrane interactions.

INTRODUCTION

Type 2 diabetes mellitus is one of the major amyloid diseases where 383 million people around the globe are suffering from this complex conformational metabolic disease [1]. The formation of extracellular amyloid aggregates composed of amylin is a major contributor to the disease and the most insoluble amyloid fibre. More than 90 % of T2DM patients have human islet amylin polypeptide (hIAPP) amyloid in their islets of Langerhans, as determined by post-mortem analysis [1-3]. The presence of islet amyloid in T2DM has been linked to the death of insulin producing β-cells, thereby contributing to the development of this disease [2-4]. Under normal physiological conditions, pro-hIAPP, a hormone of the amino acid residue in hIAPP is an insulin antagonist that is co-secreted along with insulin by pancreatic β-cells. The unspecified conformation of pro-hIAPP facilitates the formation of hIAPP fibers and this hIAPP is toxic to insulin producing β-cells [3]. For therapeutic applications, understanding the biochemical and biophysical mechanism of hIAPP is imperative and hence, the physical, chemical and biological behaviours of hIAPP *in vivo* and *in vitro* have to be investigated. Further, different models are essential to decipher the commonly observed hIAPP fibril morphologies. Previous studies have shown that the morphological character of hIAPP fibrils in pancreatic islets remain almost unaltered as observed in both *in vitro* and *in vivo* cases, evidenced by the number of protofibrils [5-7]. Because of the consumption of hIAPP oligomers during hIAPP fibril growth, oligomers were found to be on-pathway as indicated by a few researchers [8-11]. Using a therapeutic strategy based on inhibition of on-pathway hIAPP oligomers and/or fibrils is a critical issue, because the possibility of toxic off-pathway oligomers being largely populated is very high. Considering the variations observed in character and size of oligomers, it is very much likely that both on- and off-pathway hIAPP oligomers co-exist.

In spite of the above studies, structural information about hIAPP is very sparse. Monomeric hIAPP, in most of the studies were produced synthetically and the natively unfolded peptide showed rapid aggregation of monomeric hIAPP in an aqueous environment leading to the formation of insoluble fibrils in quick time. This acts as the main impediment to studying the structural characteristics of monomeric hIAPP in solution. The first observation of soluble amyloid oligomers affecting the integrity of a lipid bilayer by forming an ion-channel was made by Arispe *et al.* [12]. Later, it was shown that cation-selective channels were formed by both hIAPP and Aβ, an amyloidogenic protein associated with Alzheimer's disease [13]. Currently, a significant amount of experimental data suggests that many other amyloidic peptides and proteins form cation-selective channels [14-16]. As mystery behind the structure and formation of hIAPP oligomers continues to exist, there is a lack of information available on the secondary structure of hIAPP oligomers indicating that there is greater scope for exploratory research in these areas. In this direction, atomic force microscopy and fluorescence microscopy, among the various available techniques have been used extensively to study the interactions of fiber forming peptides [17,18] and for quantifying the interaction of amylin with bilayer. Yet, to the best of our knowledge, no study has demonstrated how it leads to amyloid fibril formation and thus leading to the complication of the disease conditions. Hence, the present study uses atomic force microscopy and fluorescence microscopy to demonstrate the interactions of non-fiber forming oligomers of amylin with lipid bilayers.

EXPERIMENTAL

Human amylin (1-37) residue containing an amidated C-terminus was purchased from GL Biochem (Shanghai) Ltd, China. The peptide was > 99 % pure and supplied as a dry powder in 0.5 mg amounts sealed in glass vials. Because the lipid is poorly soluble in water, chloroform dissolved lipids 1,2-dioleoyl-sn-glycero-3-phosphocholine (DOPC), 1,2-dipalmitoyl-sn-glycero-3-phosphocholine (DPPC), 1,2-dipalmitoyl-sn-glycero-3-phospho-(1'-rac-glycerol) (sodium salt) (DPPG) were purchased from Avanti Polar Lipids as a liquid in ordered amounts sealed in glass vials. The lipids were directly used without any further purification. Phosphate buffer saline (PBS) was prepared in the laboratory using standard procedures. Tetramethylrhodamine (TRITC) was purchased from Gene X India Bioscience Pvt. Ltd.

Preparation of lipid vesicles: The preparation of lipid vesicles was carried out with modifications as described by Richter and Brisson [19], Seu *et al.* [20], Mingeot-Leclercq *et al.* [21] and Choucair *et al.* [22]. In brief, the chloroform dissolved lipids were mixed in a 3:1 ratio, dried under a stream of N_2 gas followed by drying in a vacuum desiccator overnight to ensure that there are no traces of chloroform. The lipid mixtures were rehydrated with PBS buffer (pH 7.4), 150 μM NaCl solution and milli-Q water at 2 mg/mL final concentration. Lipid mixtures were homogenized by subsequent vortexing. Small unilamellar vesicles (SUVs) were obtained by sonication using a probe-sonicator (Ultrasonic liquid processor) operated in a pulse mode for 30 min with 10 min intervals, followed by 10-11 times of filtration using nylon syringe filters (Axiva 0.45 μm). Small unilamellar vesicle suspensions were stored at 4 °C overnight and used within 24 h.

Preparation of peptide solution: The preparation of peptide stock solution was carried out as described by Choucair *et al.* [22]. In brief, the lyophilized peptide was solubilized in DMSO at a concentration of 2 mg/mL stock solution left at 4 °C. The stock solution was utilized within 24 h. In some instances, to prevent molecular overcrowding of fluorescence and AFM scan areas, stock solutions were diluted to concentrations of 100 μM in DMSO immediately prior to imaging.

Sample preparation for fluorescence imaging: Fluorescence imaging was done as described by Choucair *et al.* [22] and Sedman *et al.* [23]. In brief, peptide stock solution (5 μL) having fluorescently labeled SUV (10 μL) was added to the micro slide and was incubated for 10 min at 25 °C. Then the slide was imaged immediately in the buffer media. The slide was rinsed to get a clear image and to remove the unaggregated hIAPP. The time lapse images were collected using SC-146Y series Epi-Fluorescence Microscope (Pulse Life Sciences, Mumbai, India), equipped with a super high mercury lamp DC 100W of excitation wave length 420-490 and 500-550 nm and a TIRF oil immersion objective. The fluorescence images were collected using a Tucsen CCD camera.

Preparation of lipid bilayers for AFM imaging: Atomic force microscopyimaging was done as described by Choucair *et al.* [22]. In brief, supported lipid bilayers were prepared using the vesicle fusion method. Briefly, to a piece of freshly cleaved mica, 10 μL SUVs (2 mg/mL) were added and allowed to settle for 10 min at 25 °C. To this, 10 μL of peptide stock solution (100 μM) was added to mica containing bilayer and later, imaging was done using an atomic force microscopy (Bruker, IISc, Bangalore, India) in tapping mode using a silica tip of 10 nm size with a force of 0.01 N/m and a resonance frequency of 20 and 25 kHz in water were used for PBS buffer wet imaging. The topographical images were analyzed using nanoscope analysis software.

RESULTS AND DISCUSSION

Type 2 diabetes mellitus (T2DM) is an amyloid disease affecting millions of people around the world in which formation of fibrillar hIAPP, is a major contributor to the disease. The unspecified conformation of hIAPP facilitates the formation of hIAPP fibrils and this hIAPP is toxic to insulin producing β-cells [3]. With regard to therapeutic implications, understanding the biochemical and biophysical mechanism of formation and interaction of hIAPP is imperative. Hence, in the present study an attempt is made to understand the mechanism/interactions involved in hIAPP oligomerization and how it interacts with ordered and disorded phase separated lipid membranes [24], upon prolonged incubation at 25 °C. It was observed that prior to peptide insertion into the membrane, no significant interaction was detected (Figs. 1a and 2a). After 45 min of peptide addition, *i.e.*, insertion of hIAPP into SUVs, the peptide seems to attain preferentially a lipid disordered phase (DOPC/DPPC) and a lipid ordered phase (DPPC/DPPG), by which the lipid bilayer morphology is subsequently affected. This is the reason behind the predominant appearance of globular hIAPP as indicated

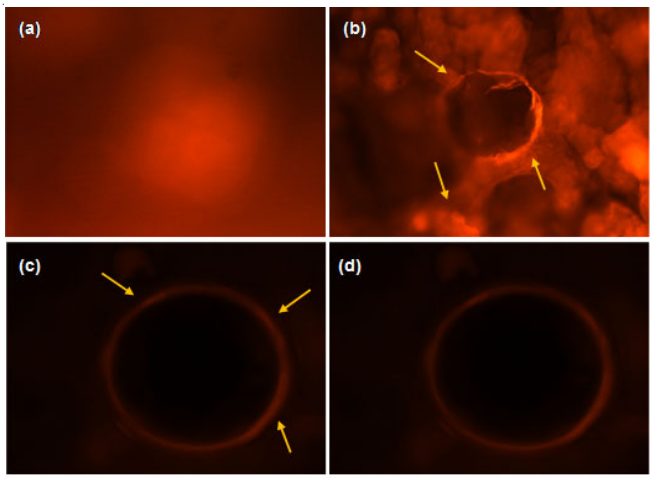

Fig. 1. Fluorescence images of DOPC/DPPC (3:1 ratio) bilayer aggregation with hIAPP. (1a) At initial time; (1b) After 45 min of incubation; (1c) After 12 h of incubation; (1d) After 24 h of incubation at 25 °C in PBS media

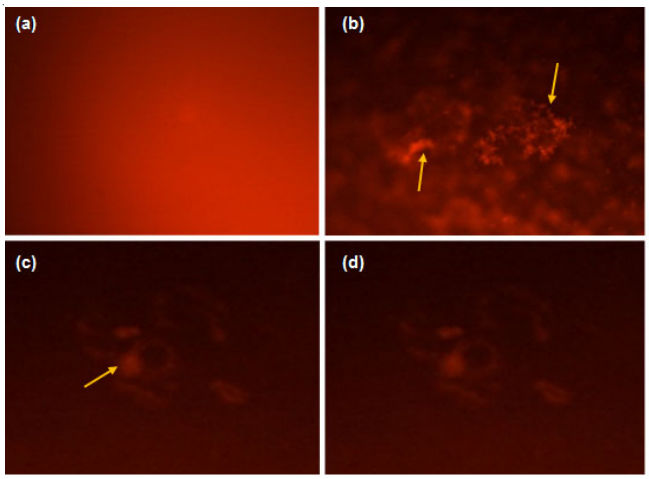

Fig. 2. Fluorescence images of DPPC/DPPG (3:1 ratio) bilayer aggregation with amylin. (2a) At initial time; (2b) After 45 min of incubation; (2c) After 12 h of incubation; (d) After 24 h of incubation at 25 °C in the PBS media

by arrows (indicated in yellow) (Figs. 1b and 2b). Further, at a concentration of 100 μM, pores were not clearly visible and hence, it is evident that they neither affected the binding nor the pore forming properties. Moreover, the indicated arrow positions in Figs. 1b and 2b disappeared after 12 h of incubation in PBS buffer at room temperature (Figs. 1c and 2c). Our time-lapse studies indicate notable changes in SUV morphologies due to strong interaction with hIAPP, especially, within the first hour of interaction. Over time, hIAPP induces detachment of stable SUVs from undergoing transformation into the growing fibrils. Therefore, aggregation of amyloid proteins on the membrane facilitates nucleation and the growth of lipid-containing amyloid aggregates (within 1 h). Later, the lipid membrane serves as a template for protein aggregation, rejecting the spherical shape and size of the template intact SUVs (globular aggregation as seen in AFM images) [25]. Small unilamellar vesicles exhibited bright spots of fluorescent lipids at specific locations as indicated by arrows on the membrane surface in the presence of hIAPP (Figs. 1c and 2c). The observed bright spots were due to the localized aggregation of peptides on the surface of SUVs [3]. Further continuing the incubation for 24 h, no unbroken SUVs were detected indicating an overall pronounced association/absorption of lipids into the growing hIAPP nonfibrils. The resultant SUVs show a decrease in the intensity (Figs. 1d and 2d), however, the lowering of intensity is due to peptide-induced lipid aggregates competing with the defect-forming activity of hIAPP [26]. Here, the fluorescent labeling suggests that this is a two component membrane system with high DOPC and DPPC ratios where selective binding takes place due to localization of the monomers and dimers of IAPP that probably start "pulling" membrane lipids into the growing oligomers accumulated at the domain boundaries and subsequently causes inflammation of the lipid domains (Figs. 1c and 2c) [18]. This reinforces localization of oligomers. In fact, hydrophilic interactions are also considered to be a major driving force in IAPP non-fibrillar formation in the presence of membranes. This plays an important role in the formation of hIAPP at the hydrophobic lipid core region. Further, head-groups also interact with hIAPP *via* charge interaction by lowering the energy barrier that eventually separates neighboring lipid molecules while allowing penetration of peptide molecules into the lipid chains [27]. This facilitates further peptide penetration leading to an increase in the local hIAPP concentration on the surface of SUVs once these hydrophilic patches of membrane lipid chains are exposed to hIAPP [27]. Thus, our study demonstrates that amyloidgenesis is a long process and the feasibility for peptide aggregation depends on the membrane property.

Real-time AFM imaging of hIAPP in PBS buffer on mica shows that hIAPP retains the globular oligomer and non-fibrillar shape. This fact was aggravated even after 12 h of incubation at 25 °C and relatively 100 μM concentration, when no fibrillar formation was detected (Figs. 3a and 4a). Further, upon incor-porating hIAPP into lipid membranes, monomeric and dimeric globular hIAPP forms stable higher order oligomers by consuming hIAPP monomers and dimmers (Figs. 3b and 4b). A similar fact was also evidenced by Fraser *et al.* [28] and Cao *et al.* [29].

These results indicate that hIAPP forms stable, possibly covalently cross-linked, trimer, tetramer and hexamer structures at the surface of the lipid bilayer [30]. hIAPP strongly affects the lipid bilayer integrity within minutes after its addition and subsequently changes the morphology of SUVs as evidenced by Figs. 1b and 2b. Consequently, the organization of amylin aggregates on mica and in planar lipid membranes bears different chemical compositions and distinct physical properties [3].

Amplitude AFM micrographs reveal structural transitions of amylin from small spherical oligomers (indicated by blue arrows) to bigger oligomers on mica over a 12 h time period (Fig. 5a). After acquiring these micrographs, the size of individual oligomers (*i.e.*, diameter and height) deposited on mica or on planar membranes were determined using the section analysis tool. Amylin aggregates revealed that the amylin non-fibrils varied by length and consistently measured 100-200 nm in width and 10-15 nm in height [Fig. 5b]. Some hIAPP oligomers were relatively short (less than 100 nm), whereas some oligomers were extended over 500 nm in length (indicated by red arrows).

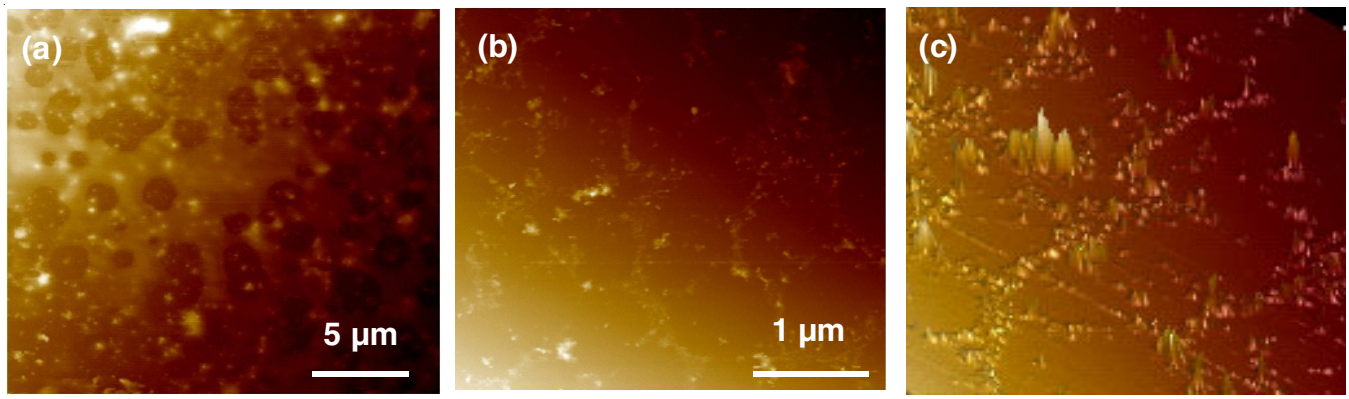

Fig. 3. Tapping mode AFM images of hIAPP peptide (100 µM) aggregated on DOPC: DPPC (3:1 ratio) bilayer incubated for 12 h. (3a) corresponds to height image; (3b) corresponds to zoomed area of 3a; (3c) is the 3D image of 3b

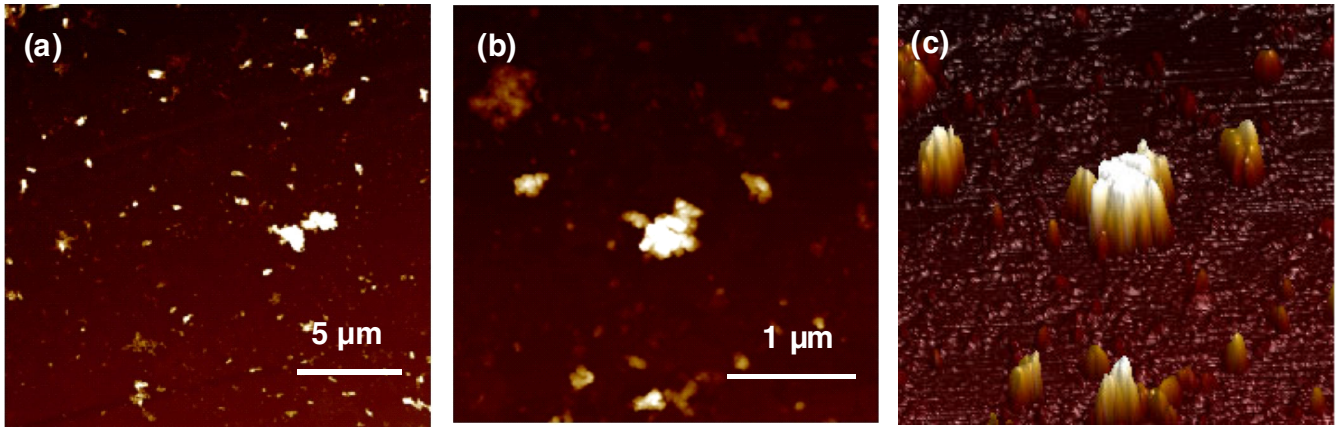

Fig. 4. Tapping mode AFM image of hIAPP peptide (100 µM) aggregated on DPPC/DPPG (3:1 ratio) bilayer incubated for 12 h. (4a) corresponds to height image; (4b) corresponds to zoomed area of 4a; (4c) is the 3D image of 4b

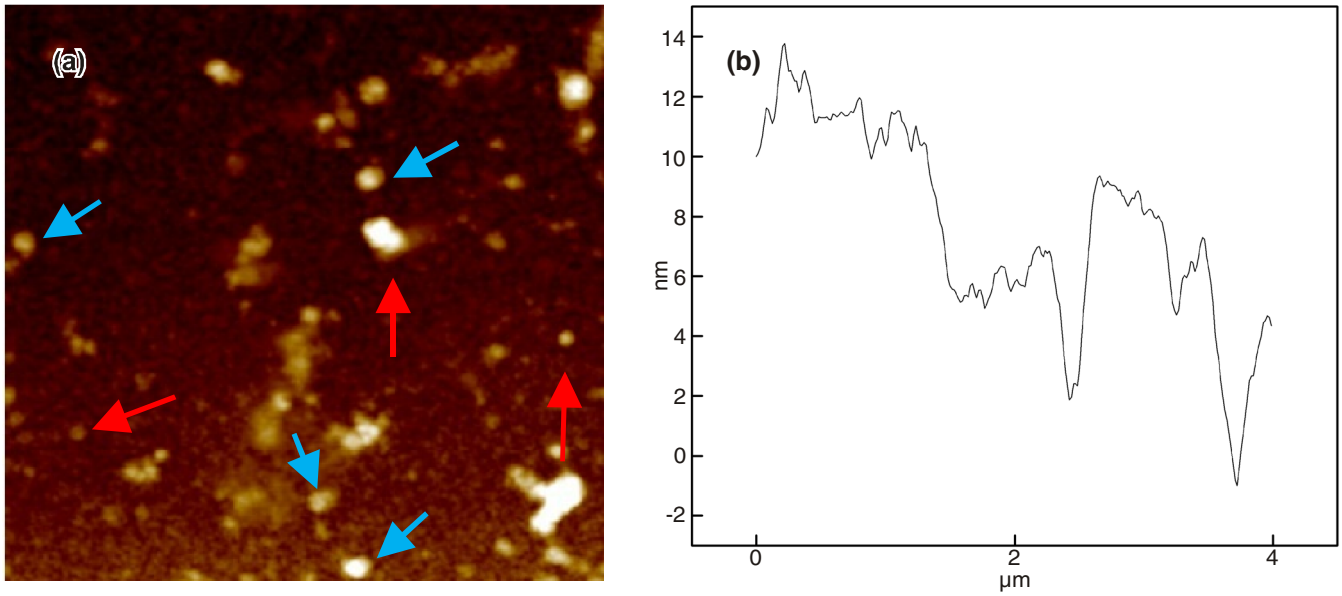

Fig. 5. AFM image of hIAPP on mica after incubation in PBS for an extended duration (5a) after 12 h and (5b) is the height profile of hIAPP on mica

The consumption of monomers and dimers leading to bigger oligomer formation after 12 h was monitored and the average size of oligomers and nonfibrils were determined using nano scope analysis. Massive amyloid-like deposits were developed after prolonged incubation that prohibits fibrillar extension. Nevertheless, AFM imaging revealed that amylin structural intermediates have a height of 15-20 nm and an average width of 100-200 nm prior to amyloid accumulation. Oligomer formation occurred in two distinct phases: initially through the deposition of small spherical oligomers and amylin

aggregation; the first phase or oligomer growth is characterized by the large change in oligomer height and width. Accordingly, our results suggest that non-fibrils are formed on mica by longitudinal extension of fully-grown oligomers rather than by lateral association of protofibrils as suggested by Parbhu *et al.* [31]. Hence, hIAPP fibrillation depends on variation in the size of building block oligomers. However, which of these two likely scenarios drives amylin aggregation in the pancreas, a lateral association of protofibrils or longitudinal extension of full width oligomers, remains unknown [17]. Moreover, the visible globular amyloid complexes were those including oligomerized amyloid that induces pathophysiological cellular activity and degeneration resulting from protein misfolding [28]. Fig. 4c showed that hIAPP aggregates at a particular spacing on the surface due to polar nature of the lipid that contributed to hIAPP oligomer interaction. Because of the lesser interfacial tension at the boundary of lipid phases and greater hydrophilic interaction, the oligomer concentration was found to be very high at the periphery. Further, changes in the lipid domain can be easily achieved by increasing the concentration of hIAPP oligomers at the boundary of lipid phase [32]. The aggregation of hIAPP also depends on the membrane. From Fig. 4c, it is clear that ordered (DPPC/DPPG) membranes strongly interact with hIAPP oligomers having a diameter of about 100 nm and a height of about 15 nm. However, in the case of disordered (DOPC/DPPC) membranes, hIAPP aggregation is less but the oligomers have a diameter of about 200 nm and a height of about 25 nm (Fig. 3c). From the above discussions, it is obvious that disordered membranes contribute to the formation of bigger hIAPP oligomers than ordered membranes.

Conclusion

One of the key elements found in the pancreatic islets of patients with T2DM is the hIAPP. The functionality and the viability of β-cells are impaired by stimulating hIAPP aggregation processes. The present article focuses on the interactions between hIAPP and lipid membranes using typical atomic force microscopy and fluorescence microscope techniques. The addition of peptide on the surface of the lipid bilayer resulted in morphological changes as revealed by both atomic force microscopy and fluorescence microscope images. Further, prologned incubation led to the formation of massive amyloid-like deposits and subsequently stable oligomeric structures. The concentration of these oligomers was found to be very high at the periphery of the membrane. Hence, with a decrease in the aggregation of hIAPP on disordered membranes, the later was found to be more influential than the ordered ones. These results strongly suggest that oligomerization leads to the pathophysiology of diabetes and not the fibrillar formation.

ACKNOWLEDGEMENTS

The authors, M.B. Divakara and M.S. Santosh, acknowledge the DST-SERB, Govt. of India for the financial support under the Fast-Track Scheme for the Young Scientists (SB/FT/CS-013/2013). Another author B.L. Dhananjaya, acknowledge the financial assistance of DST, Govt. of India for the International Grant Indo-Srilankan (DST/INT/SLP/P-007/2012, dated 5th May, 2014) and European Union for International Grant Indo-European-Marie Curie IRSES (PIRSES-GA-2013-612131, dated 15th Nov, 2014).

REFERENCES

1. P. Nedumpully-Govindan and F. Ding, *Sci. Rep.*, **5**, 8240 (2015).
2. M.F. Engel, *Chem. Phys. Lipids*, **160**, 1 (2009).
3. D. Radovan, N. Opitz and R. Winter, *FEBS Lett.*, **583**, 1439 (2009).
4. A. Clark, C.E. Lewis, A.C. Willis, G.J.S. Cooper, J.F. Morris, K.B.M. Reid and R.C. Turner, *Lancet*, **330**, 231 (1987).
5. P. Westermark, U. Engstrom, K.H. Johnson, G.T. Westermark and C. Betsholtz, *Proc. Natl. Acad. Sci. USA*, **87**, 5036 (1990).
6. E.J.P. de Koning, E.R. Morris, F.M.A. Hofhuis, G. Posthuma, J.W.M. Hoppener, J.F. Morris, P.J.A. Capel, A. Clark and J.S. Verbeek, *Proc. Natl. Acad. Sci. USA*, **91**, 8467 (1994).
7. E.T. Jaikaran and A. Clark, *Biochim. Biophys. Acta*, **1537**, 179 (2001).
8. M. Anguiano, R.J. Nowak and P.T. Lansbury, *Biochemistry*, **41**, 11338 (2002).
9. Y. Porat, S. Kolusheva, R. Jelinek and E. Gazit, *Biochemistry*, **42**, 10971 (2003).
10. J.D. Green, C. Goldsbury, J. Kistler, G.J. Cooper and U. Aebi, *J. Biol. Chem.*, **279**, 12206 (2004).
11. J.D. Knight, J.A. Hebda and A.D. Miranker, *Biochemistry*, **45**, 9496 (2006).
12. N. Arispe, E. Rojas and H.B. Pollard, *Proc. Natl. Acad. Sci. USA*, **90**, 567 (1993).
13. T.A. Mirzabekov, M.C. Lin and B.L. Kagan, *J. Biol. Chem.*, **271**, 1988 (1996).
14. M. Kawahara, Y. Kuroda, N. Arispe and E. Rojas, *J. Biol. Chem.*, **275**, 14077 (2000).
15. J.I. Kourie, A.L. Culverson, P.V. Farrelly, C.L. Henry and K.N. Laohachai, *Cell Biochem. Biophys.*, **36**, 191 (2002).
16. B.L. Kagan, R. Azimov and R. Azimova, *J. Membr. Biol.*, **202**, 1 (2004).
17. W.-J. Cho, B.P. Jena and A.M. Jeremic, *Methods Cell Biol.*, **90**, 267 (2008).
18. Y. Yu, J.A. Vroman, S.C. Bae and S. Granick, *J. Am. Chem. Soc.*, **132**, 195 (2010).
19. R.P. Richter and A. Brisson, *Langmuir*, **19**, 1632 (2003).
20. K.J. Seu, A.P. Pandey, F. Haque, E.A. Proctor, A.E. Ribbe and J.S. Hovis, *Biophys. J.*, **92**, 2445 (2007).
21. M.P. Mingeot-Leclercq, M. Deleu, R. Brasseur and Y.F. Dufrene, *Nat. Protoc.*, **3**, 1654 (2008).
22. A. Choucair, M. Chakrapani, B. Chakravarthy, J. Katsaras and L.J. Johnston, *Biochim. Biophys. Acta*, **1768**, 146 (2007).
23. V.L. Sedman, S. Allen, W.C. Chan, M.C. Davies, C.J. Roberts, S.J. Tendler and P.M. Williams, *Protein Pept. Lett.*, **12**, 79 (2005).
24. H. Himeno, N. Shimokawa, S. Komura, D. Andelman, T. Hamada and M. Takagi, *Soft Matter*, **10**, 7959 (2014).
25. E. Sparr, M.F.M. Engel, D.V. Sakharov, M. Sprong, J. Jacobs, B. de Kruijff, J.W.M. Höppener and J. Antoinette Killian, *FEBS Lett.*, **577**, 117 (2004).
26. N.B. Leite, A. Aufderhorst-Roberts, M.S. Palma, S.D. Connell, J.R. Neto and P.A. Beales, *Biophys. J.*, **109**, 936 (2015).
27. K. Weise, D. Radovan, A. Gohlke, N. Opitz and R. Winter, *ChemBioChem*, **11**, 1280 (2010).
28. P.E. Fraser, J.T. Nguyen, H. Inouye, W.K. Surewicz, D.J. Selkoe, M.B. Podlisny and D.A. Kirschner, *Biochemistry*, **31**, 10716 (1992).
29. Y. Cao, D. Hamada, Y. Kong, P. Cao, J. Guo and J. Chen, in ed.: A. Mendez-Vilas, Current Microscopy Contributions to Advances in Science and Technology, Microscopy Book Series No. 5, pp. 668-677 (2012).
30. H. Lin, R. Bhatia and R. Lal, *FASEB J.*, **15**, 2433 (2001).
31. A. Parbhu, H. Lin, J. Thimm and R. Lal, *Peptides*, **23**, 1265 (2002).
32. P.-E. Milhiet, M.-C. Giocondi, O. Baghdadi, F. Ronzon, C. Le Grimellec and B. Roux, *Single Mol.*, **3**, 135 (2002).